

MDPI

Article

Dehydrogenative Conversions of Aldehydes and Amines to Amides Catalyzed by a Nickel(II) Pincer Complex

Peter Szwedo ¹, Travis Jumper ¹, Karie Sanford ¹, Taylor Arnold ¹, Sarah Coffman ¹, Davonte Hokes ¹, Pradip Munshi ², Brian Walker ¹ and Anindya Ghosh ¹,*

- Department of Chemistry, University of Arkansas at Little Rock, 2801 South University Avenue, Little Rock, AR 72204, USA; pkszwedo@ualr.edu (P.S.); txjumper@ualr.edu (T.J.); kesanford@ualr.edu (K.S.); tearnold@uams.edu (T.A.); scoffman@uams.edu (S.C.); dfhokes@ualr.edu (D.H.); blwalker2@ualr.edu (B.W.)
- ² CISCHEM, Centre for Innovation and Sustainable Chemistry, Kalpvruksh Complex, Vadodara 390021, India; pradip.munshi@cischem.org
- * Correspondence: axghosh@ualr.edu; Tel.: +1-501-916-5197

Abstract: A C-N cross-coupling approach involving oxidative amidations of aromatic aldehydes in the presence of an amide-based nickel(II) pincer catalyst (2) is demonstrated. Upon optimization, quick reaction times (15 min) and an ideal temperature (25 °C) were established and implemented for the conversion of 33 different amide products using only 0.2 mol% of catalyst. Moderate to good turnover numbers (TONs) were obtained for secondary benzamide products, and moderate TONs were obtained for tertiary benzamide products, with the highest turnover number calculated for the 4-chloro-N-(3-phenylpropyl)benzamide product (4i, 309). Gas chromatographic–mass spectrometric (GC–MS) analysis also indicates the formation of alcohols in different reactions, indicating an oxidative amidation process. Kinetic studies were performed by varying the amount of catalyst, aldehyde, LiHMDS base, and amine substrate to determine the order of reaction for each component. Benzaldehyde and benzaldehyde- d_6 were reacted with benzylamine, and the $k_{\rm H}/k_{\rm D}$ ratio was determined to understand the rate-determining step. Isotope labeling further revealed that deuterium was being transferred to both the alcohol side product and the target amide product. With the help of kinetic data and UV–visible spectra, a mechanism for the amidation process via the catalyst (2) is proposed through a Ni(I)–Ni(III) pathway.

Keywords: amides; oxidative amidation; aldehyde; amine; nickel(ii) pincer catalyst; C-N cross-coupling



Citation: Szwedo, P.; Jumper, T.; Sanford, K.; Arnold, T.; Coffman, S.; Hokes, D.; Munshi, P.; Walker, B.; Ghosh, A. Dehydrogenative Conversions of Aldehydes and Amines to Amides Catalyzed by a Nickel(II) Pincer Complex. *Catalysts* 2023, 13, 1423. https://doi.org/ 10.3390/catal13111423

Academic Editor: Hiroto Yoshida

Received: 10 October 2023 Revised: 2 November 2023 Accepted: 3 November 2023 Published: 8 November 2023



Copyright: © 2023 by the authors. Licensee MDPI, Basel, Switzerland. This article is an open access article distributed under the terms and conditions of the Creative Commons Attribution (CC BY) license (https://creativecommons.org/licenses/by/4.0/).

1. Introduction

Amide-containing compounds are valuable organic compounds, and the demand for better access is perhaps more urgent than for any other class of chemical compounds [1]. The robust nature of substances containing amides is attributed to the stability of the amide bond [2]. Amide functionalities are essential to life processes, prevalent in natural and synthetic materials/products, and hold widespread synthetic applications [3]. The peptide bond, a type of amide linkage, is embedded within the primary structure of proteins [4]. Amides anchor the chemical structures of herbicides, such as acetochlor [5]. Formations of strong polymeric materials, such as Kevlar® and nylon, rely on repeating units of amide linkages in their structures [6]. Furthermore, amides are not only renowned for being critical precursors in organic synthesis [7] but also comprise vast numbers of critical pharmaceuticals that rely on amide bond formations. It is estimated that approximately 25% of all drugs contain amides, and amidation reactions are frequent in medicinal chemistry [8]. Amide-based medications are tailored to treat complex conditions, such as Alzheimer's, various cancers, and even HIV [9]. Academics and industrialists alike claim that countless numbers of next-generation drugs and chemicals will rely not only on amides as precursors to production but also as integral components for next-generation drugs [10]. A few of the industrially important chemicals that amides comprise are shown below in Figure 1.

Catalysts **2023**, 13, 1423 2 of 21

Figure 1. Summary of selected compounds containing the amide moiety.

Despite enormous importance, synthetic inefficiencies continue to plague chemical processes, including the formation of amide bonds. The simplest approach involves carboxylic acids and amines at higher temperatures to produce amides through dehydration. The most common conventional method for amide bond synthesis involves the activation of carboxylic acids to acid halides, esters, or anhydrides before further reacting with amines [11]. Coupling reagents, such as dicyclohexylcarbodiimide (DCC) and 1-ethyl-3-[3-dimethylaminopropyl]carbodiimide hydrochloride (EDC), are another popular amide synthesis route [12]. However, conventional methods usually require the presence of activating agents in situ, while coupling reagents are substrate-specific and stoichiometric in nature. Furthermore, these methods are tedious and waste-producing and can be expensive [13].

The demand to develop new methods for amide synthesis has led many scientists to shift their focus to catalytic approaches, particularly over the last decade [14]. Amide bonds are stable, and the formation of amide bonds via C–N coupling requires a high energy barrier to be overcome [15]. Catalysts, however, can be used to circumnavigate the high-energy barrier, and therefore, catalytic amide bond synthesis via C–N coupling can be an attractive way of making amide functionalities [16]. Over the years, researchers have developed catalytic amide bond formation via different pathways [10,14]. Carbonylative amidation of aryl halides in the presence of carbon monoxide along with a metal catalyst is an interesting pathway of amide bond formation [17]. However, the scope of these reactions is limited to aryl and heteroaryl halides and expensive catalysts and toxic gasses are necessary to complete the reactions. Other key breakthroughs for amidation reactions are the use of group IV metal salts [8,18], group V metals [19], boron [20,21], N-heterocyclic carbenes, and organocatalysts [22–28]. One attractive method of synthesizing amides is metal-catalyzed oxidative cross-coupling of aldehydes or alcohols with amines [29].

Catalysts **2023**, 13, 1423 3 of 21

In one of the earliest works in this field, Beller and co-workers used a Rh catalyst with cyclooctadiene (COD) ligand to oxidatively couple aldehydes with amines to form amide bonds [30]. The use of stoichiometric oxidants is required for most of these oxidative amidation reactions. In a seminal work, Milstein and co-workers reported a method of utilizing a ruthenium PNN pincer catalyst, which works with the release of hydrogen gas for the amidation reaction without using any additional oxidant [31].

To make the process more benign and cost-effective, it is desirable to develop catalysts involving 3d metals [32]. Metals such as cobalt, iron, and nickel are known to be less expensive and critical to life and, therefore, are seen as more viable alternatives to heavier 4d and 5d metals [33]. Nanoparticles involving Ni, Fe, and Co have been used to synthesize oxidative amidation reactions [34]. Ni catalysts have even been used to convert aliphatic and aromatic aldehydes to esters and amides [35]. Recently, nickel-photo redox catalytic amidation reactions were reported via the direct carbonylation of (hetero)aryl bromides [36]. However, many of these reactions need elevated temperatures, limiting the use of sensitive side groups. Recent protocols that involve various nickel catalysts have been developed to address these shortcomings [37-39]. Sang and colleagues managed to achieve yields of up to 98%, but the substrate scope for the amines is restricted mainly to different anilines, and the reaction time is 18 h [38]. Similarly, Goel and co-workers achieved yields up to 98%, but their reactions took place at elevated temperatures of 60 °C over a span of 8 h [39]. Nevertheless, in the pursuit of enhancing the catalytic synthesis methods for amides, it is essential to investigate synthesis techniques that operate under ambient conditions, provide a wide substrate scope, and avoid the use of toxic, costly reagents [40].

In this study, a distinct amide-based Ni(II) pincer complex (2) was used to demonstrate a novel synthetic amidation pathway shown in Figure 2. Previously, our group used this nickel(II) pincer catalyst (2) for C–C and C–N type coupling reactions involving various reagents [41–44]. However, (2) has never been used to synthesize amide bonds via C–N coupling reactions. To the best of our knowledge, we are the first group to use this catalyst for the formation of amide bonds using the pincer catalysts (2). We report a one-pot oxidative amidation by reacting various substituted benzaldehydes with primary and secondary amines for secondary and tertiary amide formations in the presence of (2) with turnover numbers (TONs) up to 309. The reactions occur at room temperature in the presence of a base and within just a few minutes.

Figure 2. (a) Structures of amide-based pincer ligand (1) and nickel (II) pincer complex (2). (b) General schematic for catalyzed amidation reactions.

Catalysts **2023**, 13, 1423 4 of 21

2. Results

2.1. Optimization of Reaction Atmosphere, Base, and Solvent

Preliminary confirmation of benzamide product formation led us to further explore benzamide formations through our unique process, and initial studies were performed to optimize the substrate scope for targeted amide formation. The focus of this study involved optimizing atmospheric, base, and solvent parameters. 4-chlorobenzaldehyde and benzylamine were selected as coupling partners for the purpose of optimization studies. Prior to ratio studies, 500 molar equivalents of both the aldehyde and amine substrates were used with respect to the nickel(II) complex (2 mg, 3.42×10^{-3} mmol). Initially, the reactions were carried out at room temperature for 3 h. However, investigations led to correcting the reaction time to 15 min, as is further discussed in the optimization of temperature and time. Minimal differences in turnover numbers (TONs) were observed for the formation of N-benzyl-4-chlorobenzamide when reacted under open air (60, entry 1, Table 1) and O₂ (60, entry 2, Table 1) atmospheres, but when an Ar atmosphere was applied for 5 min, TON drastically increased to 132 (entry 3, Table 1), implying the inert atmosphere was accentuating product formation. It is to be noted that the catalyst is sensitive to moisture, and so are the possible catalytic intermediates. When applying the Ar atmosphere for a 30 min duration, the N-benzyl-4-chlorobenzamide TON further increased to 197 (entry 4, Table 1). A variety of base and solvent combinations were attempted to reveal the ideal condition for yielding the highest amount of N-benzyl-4-chlorobenzamide formation. For our investigations, we tried different bases, such as potassium hydroxide (KOH), cesium carbonate (Cs₂CO₃), potassium-tert-butoxide (KOtBu), and LiHDMS, for the amidation reaction. KOH (entry 8, Table 1) yielded no products at all. Both Cs₂CO₃ and KO^tBu yielded products, but the TON was low (entries 9 and 10, Table 1).

Table 1. Optimization of base and solvent in the scope of *N*-benzyl-4-chlorobenzamide formation.

Entry	Ar Atmosphere	Base	Solvent	TON	GC Yield
1	^a 0 min	LiHMDS	DMSO	60 ± 1	10%
2	^b 0 min	LiHMDS	DMSO	60 ± 2	10%
3	5 min	LiHMDS	DMSO	132 ± 6	23%
4	30 min	LiHMDS	DMSO	197 ± 4	34%
5	30 min	LiHMDS	DMF	143 ± 2	24%
6	30 min	LiHMDS	1,4-dioxane	158 ± 6	27%
7	30 min	LiHMDS	THF	137 ± 1	23%
8	30 min	KOH	DMSO	0 ± 0	0%
9	30 min	Cs_2CO_3	DMSO	11 ± 2	2%
10	30 min	KO ^t Bu	DMSO	32 ± 4	5%

Conditions: Reactions were carried out with 2 (2 mg, 3.42×10^{-3} mmol), LiHDMS ($342 \mu L$, 0.342 mmol, 100 eq), 4-chlorobenzaldehye (241 mg, 1.71 mmol, 500 eq), benzylamine ($187 \mu L$, 1.71 mmol, 500 eq) in DMSO (1 mL) at room temperature for 30 min. Trials were performed in duplicates. Turnover numbers were calculated based on the moles of catalyst used and the moles of product formed, as determined from gas chromatographic–mass spectrometric (GC/MS) analyses. The internal standard method was employed, comparing the integrated peak areas of the target product with those of the internal standard, a prepared N-benzylbenzamide solution (111 mg in 1 mL methanol). The final weights of the standard, catalyst, reactant, and product were then calculated and normalized accordingly. ^a Open atmospheric conditions were implemented. ^b Pure O_2 atmosphere was applied.

Catalysts 2023, 13, 1423 5 of 21

The investigations concluded that lithium bis-(trimethylsilyl) amide (LiHMDS) was the ideal base. While the pKa of bases in DMSO plays an essential role in controlling the product yield, in the case of LiHMDS, the nature of the product reflects that nucleophilicity is likely more pronounced than basicity [45] LiHMDS is primarily used as a strong nucle-ophile rather than a base, as the pKa of the conjugate base is ~26 (less basic than lithium diisopropylamide (LDA), pKa 36) [46,47]. The pKa of LiHMDS in DMSO is 30 [48], and that of K^tOBu is 32 [49]. This clearly dictates that KO^tBu acts as a stronger base, whereas LiHMDS may act as more of a nucleophile. However, the reducing power of LiHMDS to furnish Ni catalysts suitable for catalysis at a lower valency cannot be ruled out for catalytic reactions [50].

We also checked the reactions in different solvents, such as tetrahydrofuran (THF), 1,4-dioxane, dimethylformamide (DMF), and dimethyl sulfoxide (DMSO). Interestingly, all solvents, as indicated in Table 1, yielded the products in a relatively good TON. However, DMSO was found to be the best solvent for our reactions, as indicated by the maximum TON calculated for the *N*-benzyl-4-chlorobenzamide product (197). The solvent effects could be attributed to the high solubility of the reagents, including the catalyst and the enhanced nucleophilicity that amine substrates experience in polar aprotic solvent environments, such as DMSO, as has been reported in the literature [51]. The entirety of the findings of these investigations are summarized in Table 1.

The catalyst fully dissolves, maintaining homogeneity in the system. This is crucial for considering the TON of catalytic reactions [52,53]. This is further indicated by the fact that the catalyst goes into the solution, and the solution does not become turbid. Moreover, the consistency of the solution is preserved upon filtration.

2.2. Optimization of Temperature and Time

The oxidative amidation reactions of 4-chlorobenzaldehyde and benzylamine to N-benzyl-4-chlorobenzamide at different time increments were evaluated at different temperatures based on the TONs. The measurements were taken at 25 °C, 70 °C, and 110 °C. It is worth noting that the highest rate of benzamide formation was observed within the first 5 min, while a significant rate of formation was observed for an additional 10 min following this initial period. The studies reveal that lower N-benzyl-4-chlorobenzamide TONs are experienced when temperature is increased. The maximum conversions of benzamide formations were measured at 25 °C, while the minimum TON measured occurred at the highest temperature, 110 °C. After approximately 15 min, the minimal benzamide product was observed to be formed, suggesting that the reaction was saturated with the benzamide product. Nevertheless, the reaction was carried out for 15 min for good measure. The temperature effects on benzamide yields suggest that this process maintains an exothermic nature as added heat attenuates the amide product formation. The optimal temperature and time for these reactions were thus established at 25 °C for 15 min, respectively. The entirety of the findings of these investigations are summarized in Figure 3a.

2.3. Optimization of Starting Reagent Ratios

The effect of varying the molar ratios of 4-chlorobenzaldehyde and benzylamine was examined using LiHMDS as the base and DMSO as the solvent. The studies were performed at $25\,^{\circ}$ C, and 500 molar equivalents with respect to the catalyst load was used as the baseline amount to produce three comparisons. The lowest TON is marked by the reaction involving 1000 equivalents of the amine and 500 equivalents of the aldehyde. The intermediate TON involved equimolar amounts of aldehyde and amine substrates, both at 500 equivalents. The highest TON involved doubling the amount of the aldehyde to 1000 equivalents while maintaining 500 equivalents of the amine substrate. The results of these investigations proved fruitful as the net TON of the formed *N*-benzyl-4-chlorobenzamide considerably increased (3c, 237). In all cases, considerable amide TONs were produced, but it was ultimately determined to double the amount of aldehyde substrate with respect to the amine, which ultimately produces the maximum amount of benzamide product. This can

Catalysts **2023**, 13, 1423 6 of 21

be attributed to the flexibility, which is afforded to side-product formations, particularly in the scope of 4-chlorobenzyl alcohol (6aa), which strains the capacity of benzamide product formation, which is further evaluated in specificity investigations. The entirety of the findings of these investigations are summarized in Figure 3b.

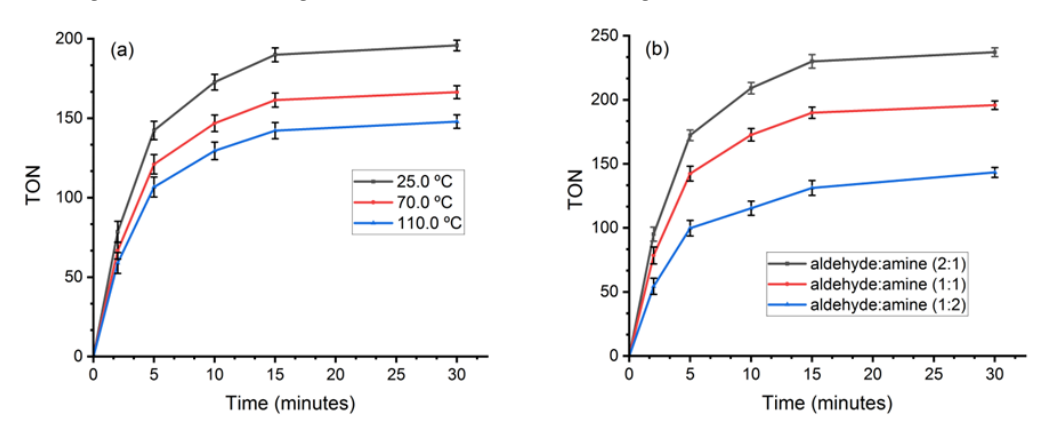


Figure 3. (a) Effects of temperature with respect to the scope of *N*-benzyl-4 chlorobenzamide turnover number (TON) formation as a function of time. **(b)** Effects of varying recant ratios in the scope of *N*-benzyl-4-chlorobenzamide TON formation as a function of time. Conditions: Reactions for temperature studies were carried out with 2 (2 mg, 3.42×10^{-3} mmol), LiHDMS (342 μL, 0.342 mmol, 100 eq), 4-chlorobenzaldehye (481 mg, 3.42 mmol, 1000 eq), benzylamine (187 μL, 1.71 mmol, 500 eq) in DMSO (2 mL) at room temperature (r.t.). for 30 min. Reactions for ratio studies were carried out with 2 (2 mg, 3.42×10^{-3} mmol), LiHDMS (342 μL, 0.342 mmol, 100 eq), 4-chlorobenzaldehye (481 mg, 3.42 mmol, 1000 eq; 241 mg, 1.71 mmol, 500 eq), benzylamine (187 μL, 1.71 mmol, 500 eq; 374 μL, 3.42 mmol, 1000 eq) in DMSO (2 mL) at r.t. for 30 min. TONs were calculated based on the moles of catalyst used and the moles of product formed, as determined from gas chromatographymass spectrometry (GC/MS) analyses. The internal standard method was employed, comparing the integrated peak areas of the target product with those of the internal standard, a prepared *N*-benzylbenzamide solution (111 mg in 1 mL methanol).

2.4. Amidations in the Scope of Coupling Substituted Aromatic Aldehydes with Benzylamine

The effect of various aryl aldehydes was examined by the reaction with benzylamine, and TON was calculated for various benzyl-N-benzamide products, as summarized in Scheme 1. Turnover amounts (TONs) are indicated below each product label. Generally, moderate to good TON values were calculated (3b, 120-3c, 259). Most of the benzaldehyde starting reagents were para-substituted groups apart from one ortho-substituted electronreleasing methyl group. The electronic effect of the substituents—whether they are electron releasing or electron withdrawing—certainly affects the product formations [54]. The trend is best seen with respect to the halogenated substituents. Halogens can behave as electron donors or acceptors but, in this case, most likely are acting as π -electron donors in the para position through positive resonance contribution (+R effect) into the benzene ring [55]. This effect could change the reactivity of the C-H on the aldehyde group. N-benzyl-4fluorobenzamide (3b, 259) demonstrated the highest product formation, most likely due to fluorine's short bond length accentuating fluorine's π -electron donation capacity into the benzene ring (+R effect) [56]. N-benzyl-4-chlorobenzamide (3c, 237) exhibited the next highest conversion, as the chlorine is next to the fluorine on the +R effect. The same reason could exist for bromine as well. Noticeably, the lowest performance of -NO₂ could only be explained by its -R effect. The -OH group (3g) shows a slightly lower TON, even though the phenolic group is electron-releasing. This could be attributed to the fact that the phenolic proton can neutralize LiHDMS and, to an extent, lower the effectiveness of the base. In all, seven different benzylbenzamide products were formed, demonstrating that aryl aldehydes and benzylamine are excellent coupling partners for amide bond formation. Catalysts **2023**, 13, 1423 7 of 21

Scheme 1. Summary of amidation reactions involving benzylamine and various aryl aldehydes. Conditions: Reactions were carried out with 2 (2 mg, 3.42×10^{-3} mmol), LiHDMS (342 μ L, 0.342 mmol, 100 eq), substituted benzaldehyde (3.42 mmol, 1000 eq), benzylamine (187 μ L, 1.71 mmol, 500 eq) in DMSO (2 mL) at room temperature for 30 min. Turnover numbers were calculated based on the moles of catalyst used and the moles of product formed, as determined from gas chromatography—mass spectrometry analyses. The internal standard method was employed, comparing the integrated peak areas of the target product with those of the internal standard, a prepared *N*-benzylbenzamide solution (111 mg in 1 mL methanol).

2.5. Amidations in the Scope of Coupling 4-Chlorobenzaldehyde with Various Primary (1°) Amine Partners

Reactions involving the 4-chlorobenzaldehyde substrate and various 1° amine nucleophiles as coupling partners were then investigated. The various alkyl and aromatically substituted secondary benzamide products are summarized in Scheme 2 below. In all, sixteen different products were characterized quantitatively via GC/MS. The products obtained showed moderate to good TONs (4a, 51–4o, 309). The trend observed for 4chlorobenzylaldehyde and various non-branched aliphatic-type amine-coupled products (4a-4i) demonstrated higher amide product conversions with increasing lengths of the carbon chain. This can be attributed to the increasing nucleophilic strength of the aminecoupling partner with a longer carbon chain due to the electronic inductive effects and flexibility of the chain with enhanced entropy [57], which may affect the overall yield of the reaction. Unsurprisingly, the lowest and highest TONs recorded in this context of these reactions are attributed to 4-chloro-N-ethylbenzamide (4a, 51) and to 4-chloro-Ndecylbenzamide (4i, 214). This can be attributed to the increasing nucleophilic strength of primary amines as the carbon chain lengthens [58]. Branched alkyl amine also showed good reactivity (4j, 168). Furthermore, substituted aromatic amines were also demonstrated to be excellent reagents for 4-chlorobenzaldehyde (4l-4p). Interestingly, the highest TON value recorded in the scope of this study was measured for target product 4-chloro-N-(3phenylpropyl)benzamide (40, 309). This is due to both the ideal steric environment and

Catalysts **2023**, 13, 1423 8 of 21

nucleophilicity of this substituted amine substrate, whose reactivity is further pronounced by the aliphatic chain connecting the benzene ring and the amine functionality. A slightly lower yield for 4j and 4h can be correlated with the steric hindrance associated with the aromatic amines. Before, we mentioned a comparison of our data to previously published works. As we found, the TON value for product 4k in our work was 210, whereas the same product reported by Goel and colleagues' work registered a TON value of 25 [39] indicating a high efficiency of the catalyst.

Scheme 2. Summary of C–N cross-coupling products for reactions involving 4-chlorobenzaldehyde and various 1° amine partners. Conditions: Reactions were carried out with 2 (2 mg, 3.42×10^{-3} mmol), LiHDMS (342 μ L, 0.342 mmol, 100 eq), 4-chlorobenzaldehye (481 mg, 3.42 mmol, 1000 eq), substituted amine (1.71 mmol, 500 eq) in DMSO (2 mL) at room temperature for 30 min. Turnover numbers (TONs) were calculated based on the moles of catalyst used and the moles of product formed, as determined from gas chromatography–mass spectrometry GC/MS analyses. The internal standard method was employed, comparing the integrated peak areas of the target product with those of the internal standard, a prepared *N*-benzylbenzamide solution (111 mg in 1 mL methanol).

Catalysts **2023**, 13, 1423 9 of 21

2.6. Amidations in the Scope of Coupling 4-Chlorobenzaldhyde with Various Secondary (2°) Amines

Reactions involving the 4-chlorobenzaldehyde and various 2° amines were then investigated. C-N cross coupling in the context of amide formation has been challenging and limited in the scope of substrate selectivity [8,59,60], but this nickel(II) complex (2) demonstrated the unique capability with 1° and 2° amines and aldehyde partners. The tertiary benzamide products obtained by the catalytic pathway are summarized in Scheme 3. The TONs obtained ranged from 19–149 (5b and 5d respectively). The lowered conversion of 2° amines in comparison to 1° amines can be attributed to steric hindrance, nucleophilicity, and enhanced N-H bond strength of the substituted amines [61]. The trend in this set of products is most apparent when comparing the TONs of 4-chloro-N,N-dibutylbenzamide (5a, 57), 4-chloro-N,N-dipentylbenzamide (5b, 44), and 4-chloro-N,N-dihexylbenzamide (5c, 38). Further, this trend is reinforced with the TONs of 4-chloro-N-ethyl-N-methylbenzamide (5e, 106), 4-chloro-N-butyl-N-methylbenzamide (5f, 66), 4-chloro-N-pentyl-N-methylbenzamide (5g, 54), and 4-chloro-N-hexyl-N-methylbenzamide (5h, 40). In the context of these benzamide products, the increasing size of alkyl substituents on the 2° amine nucleophile substrates translated to lower TON conversions for the obtained tertiary benzamides. The lowest TON resulted from the reaction involving the N-ethylpropylamine fragment (5b, 19). The highest TON was attributed to the product resulting from the reaction involving morpholine (5d, 149).

Scheme 3. Summary of C–N cross-coupling products for reactions involving 4-chlorobenzaldehyde and various 2° amine partners. Conditions: Reactions were carried out with 2 (2 mg, 3.42×10^{-3} mmol), LiHDMS (342 μ L, 0.342 mmol, 100 eq), 4-chlorobenzaldehye (481 mg, 3.42 mmol, 1000 eq), substituted amine (1.71 mmol, 500 eq) in DMSO (2 mL) at room temperature for 30 min. Turnover numbers were calculated based on the moles of catalyst used and the moles of product formed, as determined from gas chromatography–mass spectrometry analyses. The internal standard method was employed, comparing the integrated peak areas of the target product with those of the internal standard, a prepared N-benzylbenzamide solution (111 mg in 1 mL methanol).

2.7. Evaluation of Side Product Formation and Specificity

In addition to the targeted benzamide products, considerable amounts of chlorobenzyl alcohol formations (Supplementary Materials, S68) were observed during these reactions. Organic reactions involving the reduction of aldehydes to primary alcohols are known to take place when strong reducing agents, such as lithium aluminum hydride or sodium borohydride, are used [62,63]. Interestingly, no reducing agents were implemented for these reactions, yet considerable TONs of the alcohol were observed. It is important to note that when these reactions were attempted using benzyl alcohols and amines as potential coupling partners, no formed products were observed. This suggests that the benzyl alcohol formation is inevitable and does not function as a reactant or intermediate, which is an important clue to the mechanistic pathway for this process. Furthermore, this phenomenon offers an explanation as to why lower aldehyde substrate loads restrict the optimal formation of the targeted benzamide product. Interestingly, this process revealed almost no benzyl alcohol formations after the initial five minutes. A summary of the major products is shown in Figure 4.

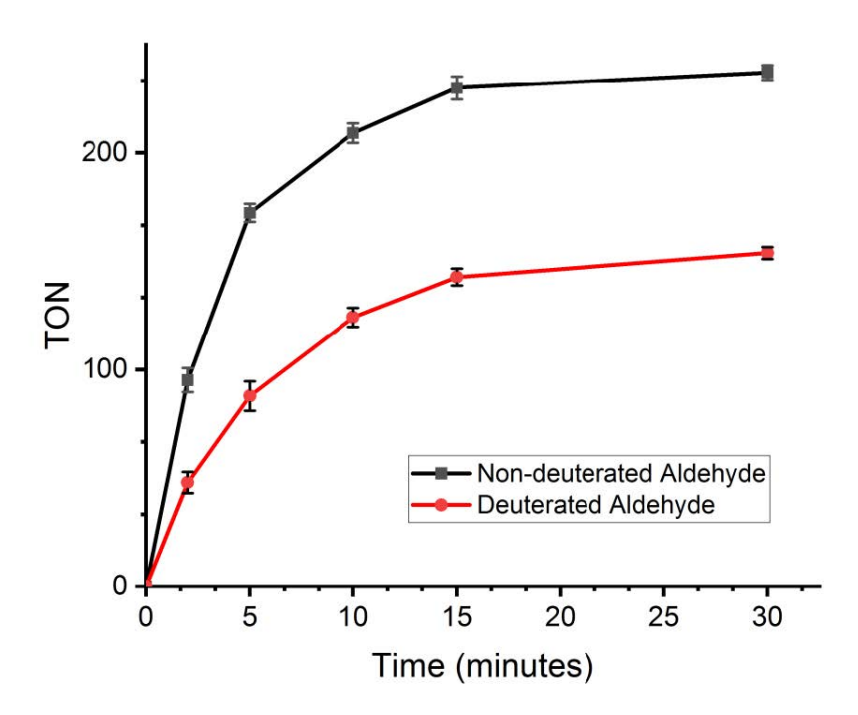


Figure 4. Overlay of major product formation with respect to time. Conditions: Reactions were carried out with 2 (2 mg, 3.42×10^{-3} mmol), LiHDMS (342 μ L, 0.342 mmol, 100 eq), 4-chlorobenzaldehye (481 mg, 3.42 mmol, 1000 eq), benzylamine (187 μ L, 1.71 mmol, 500 eq) in DMSO (1 mL) at room temperature for 30 min. Turnover numbers (TONs) were calculated based on the moles of catalyst used and the moles of product formed, as determined from gas chromatography–mass spectrometry analyses. The internal standard method was employed, comparing the integrated peak areas of the target product with those of the internal standard, a prepared *N*-benzylbenzamide solution (111 mg in 1 mL methanol).

Catalysts 2023, 13, 1423 11 of 21

It should be noted that when these reactions were also attempted using aliphatic-type aldehydes, no products were observed. It is surmised that aliphatic aldehydes are susceptible to β-hydrogen elimination and are thus not suitable to be converted to the target benzamide. Further, aniline failed to react with benzaldehyde substrates, most likely due to their profoundly less pronounced nucleophilic nature in comparison to the other amine substrates. Lastly, reactions involving carboxylic acids and ester fragments as potential amine coupling partners were also attempted, but no formed products were observed.

It is worthwhile to mention that we have not investigated the byproduct formation of which side or parallel reactions could not be ruled out; however, the proposed mechanism dictates the specific nature of the reactions toward the desired product by minimizing the byproduct formation.

2.8. Reaction Kinetics

Initial rates of amidations with respect to 4-chlorobenzaldehyde, benzylamine, Li-HDMS, and catalyst (2) were measured with respect to each other by varying the amount of one of the starting materials to determine reaction kinetics. The studies conducted involved varying the concentrations of one of these reagents while maintaining the same concentrations described in the optimized reaction conditions of the other three starting materials. The data are representative of the first 5 min for each of the amidation reactions. Plots for each of the scenarios are demonstrated in Figure 5 as the log of the rate as a function of the log of the concentration.

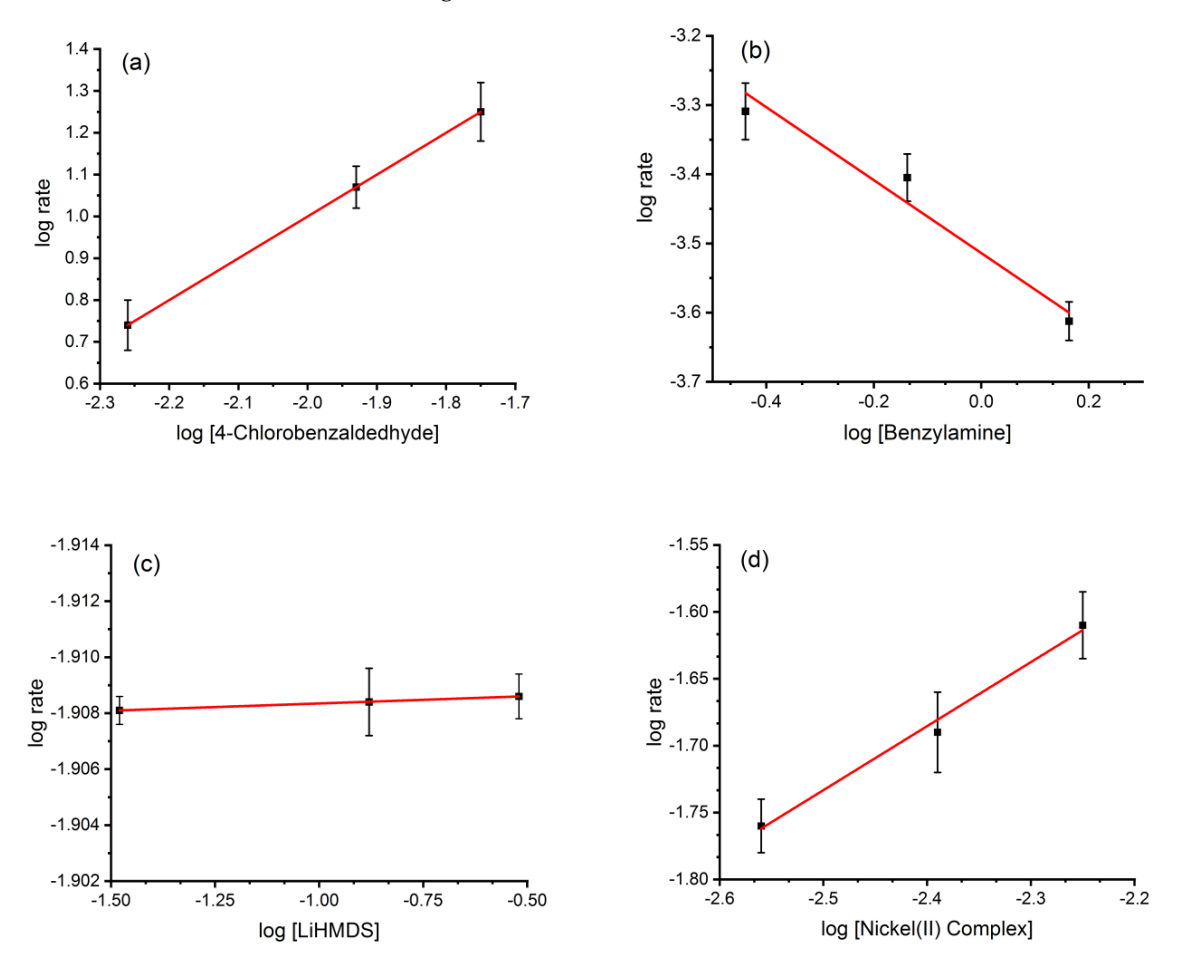


Figure 5. Plots of log rate as a function of the log of concentrations varied. (a) Log rate versus varying log [4-Chlorobenzaldehyde], maintaining all other concentrations constant. (b) Log rate versus varying log [benzylamine], maintaining all other concentrations constant. (c) Log rate versus varying log [LiHMDS], maintaining all other concentrations constant. (d) Log rate versus varying log [Nickel(II) Complex], maintaining all other concentrations constant.

Applying different rate laws provided insight into the order with respect to each of the starting reagents. With respect to the amine (benzylamine), the order is shown to be negative one-half, as is indicated by the slope of the line. With respect to the base (LiHDMS), the order is shown to be zero, as indicated by the slope. With respect to the aldehyde (4-chlorobenzaldehyde) and the catalyst (2), first-order behavior was observed. The results are consistent with literature values reported previously with other nickel complexes [64].

To further shed light on the reaction mechanisms, next, the kinetic isotope effect (KIE) was evaluated. For this study, two different time trials using benzaldehyde and benzaldehyde- d_6 were run for comparison, while all other starting reagents remained the same. Due to the haste of the initial conversion, the first 6 min were evaluated. The competitive series for the kinetic isotope effect is shown in Figure 6. According to the competitive series evaluation, the $k_{\rm H}/k_{\rm D}$ ratio was calculated to be 5.8 from the respective slopes. The high $k_{\rm H}/k_{\rm D}$ ratio is indicative that the KIE is primary for the breaking of the C–H bond, and it is therefore suggestive that the rate-determining step is the C–H bond activation step.

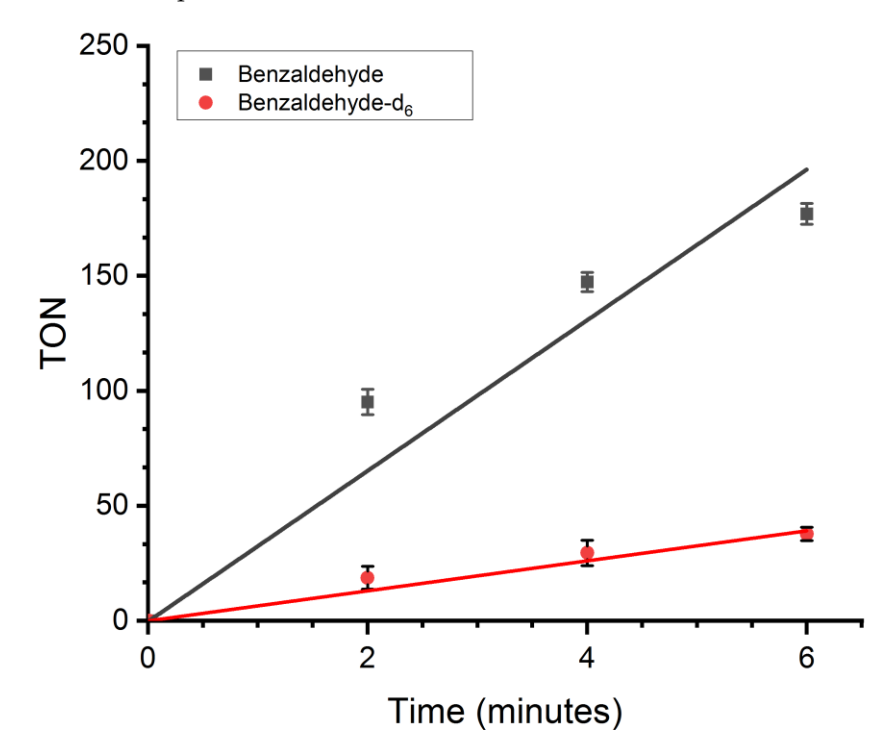


Figure 6. A comparative time study of turnover numbers (TON) for the formation of non-deuterated versus deuterated 4-chlorobenzaldehyde. The kinetic isotope effect was determined by taking the ratio of the slope of the non-deuterated aldehyde and the deuterated aldehyde. Conditions: Reactions were carried out with 2 (2.0 mg, 3.42×10^{-3} mmol), LiHDMS (342.0 μ L, 0.342 mmol, 100 eq), benzaldehyde (374.0 μ L, 3.42 mmol, 1000 eq), benzaldehyde- d_6 (348.0 μ L, 3.42 mmol, 1000 eq), or benzylamine (187.0 μ L, 1.71 mmol, 500 eq) in DMSO (2.0 mL) at room temperature for 30 min. TONs were calculated from moles of catalyst used, and the moles of product formed were obtained from gas chromatography–mass spectrometry analyses via the internal standard method, which compared integrated peak areas of the target product and the internal standard, a prepared *N*-benzylbenzamide solution (111 mg in 1 mL methanol).

2.9. Determination of Thermodynamic Parameters at the Transition State

Further, thermodynamic parameters during the transition state were evaluated. Target product conversion amounts in terms of molar concentration at 30 min were used to determine the rate constant (k) at various temperatures (25 $^{\circ}$ C, 70 $^{\circ}$ C, and 110 $^{\circ}$ C). An Eyring plot was then constructed by the natural log of the quotient of rate constant (k) and temperature in Kelvin as a function of the inverse temperature in Kelvin. The plot was then

used to calculate the change in enthalpy of activation (ΔH^{\ddagger}), entropy of activation (ΔS^{\ddagger}), and Gibbs free energy of activation (ΔG^{\ddagger}). The Eyring plot is provided below in Figure 7.

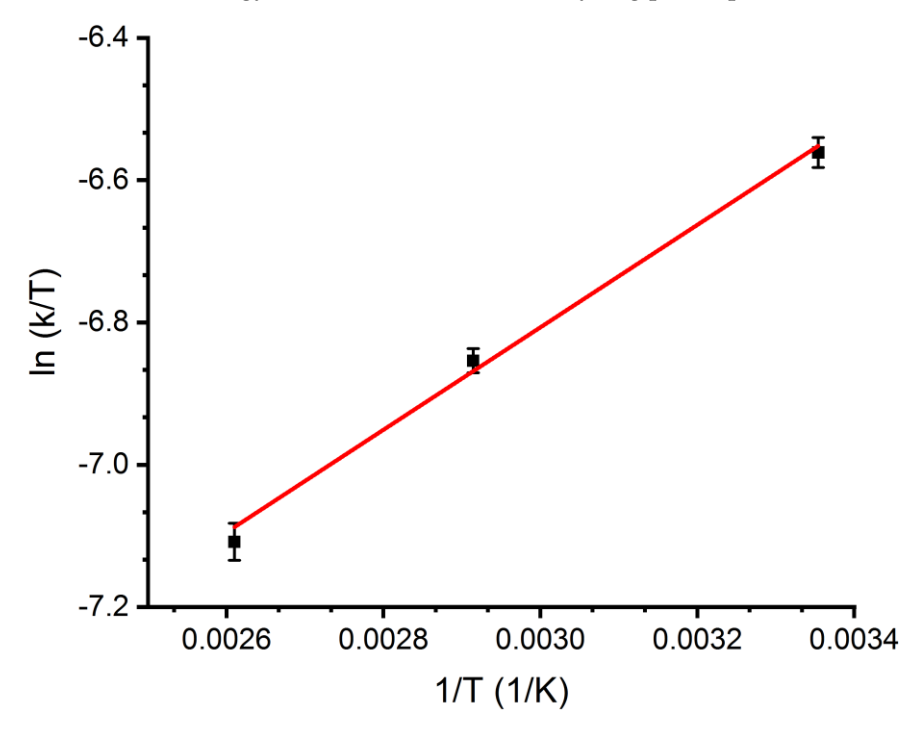


Figure 7. Eyring plot showing the natural log of the quotient of rate constant (k) and temperature (T) in Kelvin as a function of inverse T in Kelvin.

According to the plot, a positive slope and negative y-intercept were observed and were consistent with an increase in rates of reaction as the temperature decreased [65]. From the value of the slope, ΔH^{\ddagger} was determined to be -86.61 J/mol. From the value of the y-intercept, ΔS^{\ddagger} was determined to be -3.94 J/mol. ΔG^{\ddagger} was then conveniently calculated to be +1.1, +1.3, and +1.4 KJ/mol at 25 °C, 70 °C, and 110 °C respectively. Thus, the calculations indicate that the process is exothermic, becomes more ordered, and is endergonic at all temperatures measured during activation.

2.10. Proposed Reaction Pathway

Nickel complexes are known to expand oxidation states from $\mathrm{Ni^{0}}$ to $\mathrm{Ni^{IV}}$, which makes the mechanistic cycles of nickel complexes more versatile than those of palladium and platinum [66]. The divalent nickel(II) complex (2) was formed with two deprotonated σ -donating amides coordinated with the metal ion. However, such a nickel(II) complex is unlikely to be stable [67–71]. Compound 2 was synthesized using n-butyllithium, with additional $\mathrm{Li^{+}}$ obtained from the LiHMDS catalyst. This compound, 2, facilitates the amidation reactions when LiHMDS is present. $\mathrm{Li^{+}}$, due to its smaller relative size, coordinates with oxygen donor atoms. Due to the presence of excess $\mathrm{Li^{+}}$, it is possible that 2 holds an imine type coordinated with the nickel(II) complex, and it may be that both amide bonds in 2 are in the imine form. Reports of such structures can be found in the literature [72]. Therefore, it is possible that 2 is being forced into an imine-like functionality and $\mathrm{Li^{+}}$ is being coordinated with the amide oxygens. Previous literature has provided NMR evidence such a structure possibly manifested due to asymmetry in the ligand structure [73].

UV–vis spectroscopy was used to study the interaction of 2 with various substrates and starting materials. Figure 8 summarizes the effect on absorbance when the nickel(II) complex (2) is mixed with various starting materials. The catalyst alone shows absorption at 430 nm with a shoulder at 475 nm. When the aldehyde is mixed with the nickel complex, the absorbance curve looks very similar to the absorbance curve of 2, suggesting no interaction of 2 with aldehyde. When the amine is mixed with the nickel complex (2),

the absorbance spectrum peak shifts dramatically to a lower wavelength at 415 nm with a shoulder at 430 nm. This indicates the strong interaction of amine with 2. In the case when LiHDMS is mixed with 2, an absorption peak emerges, as shown at 500 nm. This is crucial for the catalytic reaction. Compound 2, when mixed with LiHDMS first and then either with benzaldehyde or benzylamine, shows similar UV–vis spectra. When 2 reacted with LiHDMS, benzaldehyde, and benzylamine, the UV–vis spectrum was then slightly changed. The key observation was the change of UV–vis upon the addition of LiHDMS. We believe the sterically hindered base reduced the Ni^{II} in 2 to low-valent Ni^I [74]. Further, our observations during the reaction process indicated that when the amine is mixed prior to the aldehyde, the reaction does not proceed, leading us to believe that the initial 2 and aldehyde interaction is the pivotal first step to the catalytic cycle.

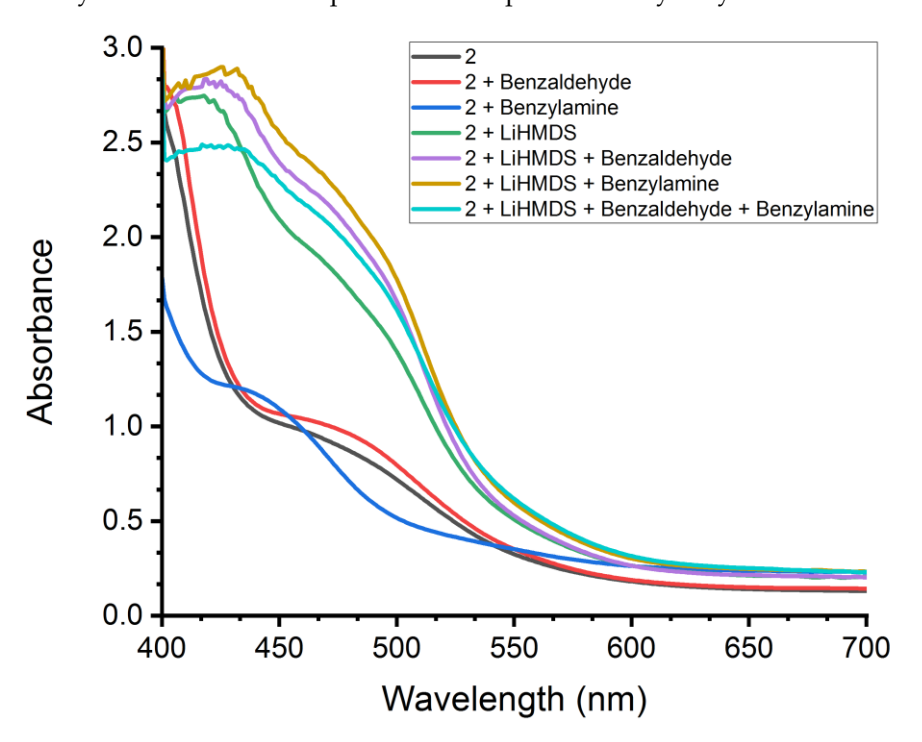


Figure 8. Ultraviolet–visible spectroscopy studies of absorbance at various wavelengths when various starting materials are mixed with nickel(II) pincer complex. Conditions: Reactions were carried out with 2 (2 mg, 3.42×10^{-3} mmol), LiHDMS (342 μ L, 0.342 mmol, 100 eq), benzaldehyde (374 μ L, 3.42 mmol, 1000 eq), benzaldehyde- d_6 (348 μ L, 3.42 mmol, 1000 eq), or benzylamine (187 μ L, 1.71 mmol, 500 eq) in DMSO (2 mL).

Thus, it is hypothesized that once the nickel(II) complex (2) is reduced, the chlorine ligand is replaced, and (2) is coordinated to the π -bond of the carbonyl on the aldehyde (2z1). This step then primes the catalyst's proton transfer capabilities. C-H bond activation then occurs via proton transfer, directing an oxidative addition forming a Ni^{III} acyl hydride intermediate (2z2). According to the k_H/k_D ratio calculated at 5.8, the C-H bond activation step serves as the rate-determining step. A second aldehyde molecule then inserts itself into the cycle, facilitating another oxidative addition while directing the formation of a meta-stable Ni^{III} acyl, alkoxy intermediate (2z3) [75]. This short-lived intermediate was not possible to characterize. It is hypothesized that this intermediate is for directing hydride shifts that generate the alcohol side-products. This may be attributed to the dual role that benzaldehydes serve as (sacrificial) acceptors for hydrogens and the substrates necessary to carry out the reaction [35]. Rearrangement is facilitated via a nucleophilic attack by the amine nucleophile. In a concerted process, a hydride shift occurs from the amine nucleophile to the alkoxy-oxygen intermediate, expelling an alcohol product while forming a Ni^{III} acyl amino intermediate (2z4). This action is supported by the formation of benzyl alcohol (6aa), confirmed through GC-MS analysis. The rapid transfer of hydrogen from Catalysts **2023**, 13, 1423 15 of 21

the amine nucleophile to form the corresponding benzyl alcohol is further reinforced by GC–MS data from the $k_{\rm H}/k_{\rm D}$ studies, as the formed benzyl alcohol gained a seventh deuterium according to the mass spectrum (Supplementary Materials, S68). Next, reductive elimination occurs from a third aldehyde entering the catalytic cycle. During this step, the final benzamide product is expelled, and the oxidation state of the complex converts from $Ni^{\rm III}$ to the original $Ni^{\rm I}$ oxidation state, and the initial $Ni^{\rm I}$ η^2 -carbonyl attachment is returned, recommencing the catalytic cycle. With the results obtained so far and the mechanism best understood by us for this amidation process, the plausible mechanism is illustrated below in Figure 9.

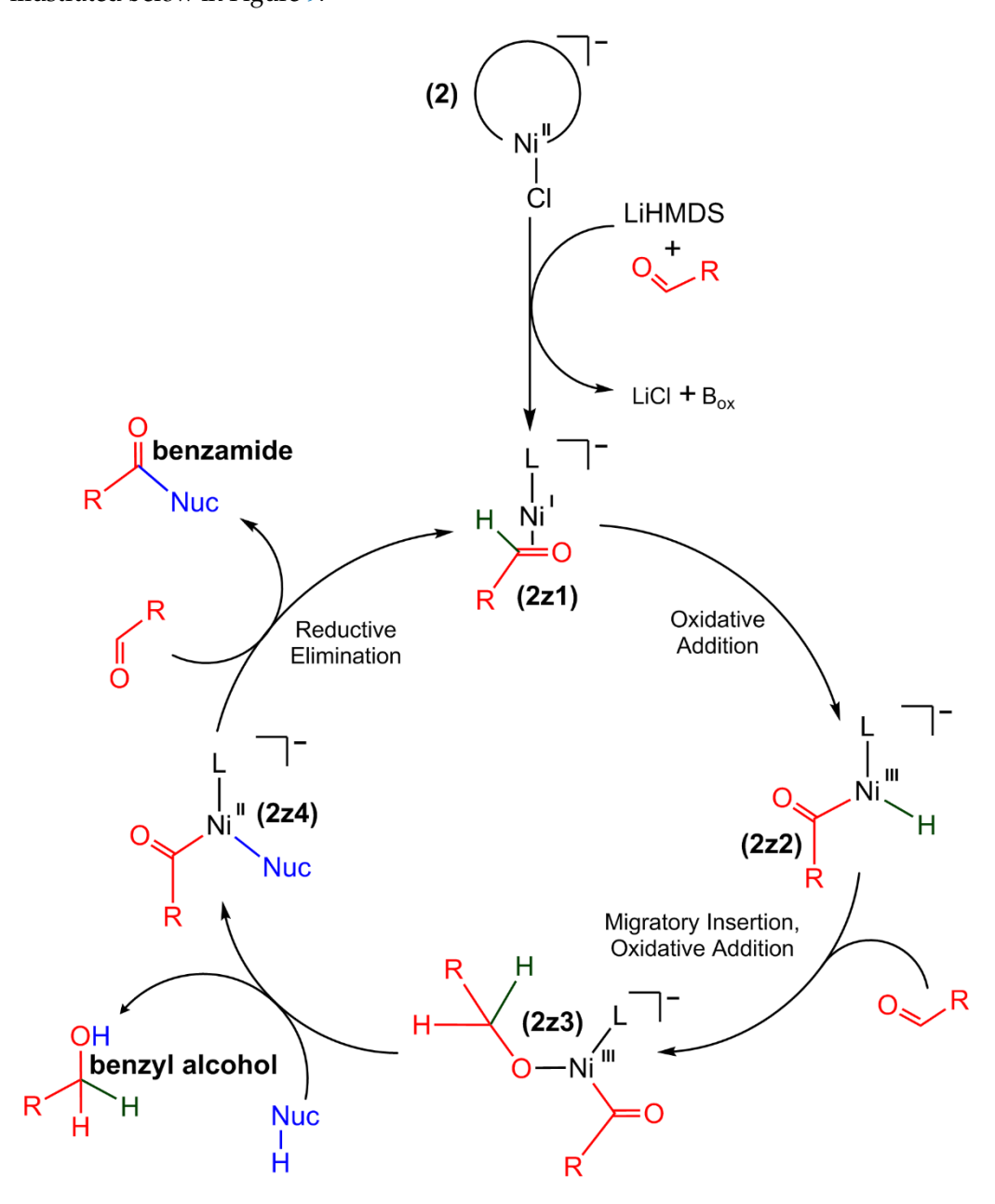


Figure 9. Proposed mechanism for nickel catalyzed (2) amidations from coupling of aryl aldehydes and various amine nucleophiles. $B_{ox} = \text{oxidized product}$.

3. Discussion

A dehydrogenative C–N cross-coupling process via a nickel(II) pincer complex (2) was demonstrated. Optimization studies showed that amide formations performed best at room temperature under argon atmosphere conditions in conjunction with DMSO as the

Catalysts 2023, 13, 1423 16 of 21

solvent and LiHMDS as a base. The nickel(II) pincer complex (2) demonstrated selectivity for facilitating oxidative amidations of aryl aldehydes to both 1° and 2° amines. Various benzaldehydes were reacted with benzylamine and successfully converted to nine different target benzaldehyde products. 4-chlorobenzaldehyde was demonstrated to be the most ideal aldehyde-coupling partner and was further utilized to react with 24 other 1° and 2° amines. For the 4-chlorobenzaldehyde 1° amine coupling partners, 16 different 2° benzamide products were obtained, and both alkyl and aromatically substituted types were shown to be excellent coupling partners. For the 2° amine coupling partners, eight different 3° benzamide products were obtained. Data analysis also indicated formations of benzyl alcohol side-products. Increasing amounts of aldehyde substrates with respect to the amine reagent enhanced benzamide formation.

Furthermore, kinetic studies revealed that the amine substrates are negative one-half order, the base is zero order, and the nickel(II) complex (2) and the aldehyde substrates are second order. KIE studies were performed, and a $k_{\rm H}/k_{\rm D}$ was calculated to be 5.8, suggesting that C–H bond activation is the rate-determining step. An Eyring plot was constructed to evaluate thermodynamic parameters at activation and were calculated to be -86.61 Joules per mole for ΔH^{\ddagger} , -3.94 J/mol for ΔS^{\ddagger} , and +1.1, +1.3, and +1.4 KJ/mol at 25 °C, 70 °C, and 110 °C, respectively, for ΔG^{\ddagger} indicating an endergonic, exothermic, and more ordered process during activation. A mechanism was proposed, and various stages of the mechanism were substantiated via UV–vis and GC–MS characterizations. It is worth noting that among the several bases tested, LiHDMS outperformed others like KOH, Cs₂CO₃, or KO[†]Bu. This opens the door for future studies aimed at developing a more cost-effective base to make the process more economical.

4. Materials and Methods

4.1. Materials

All chemicals were purchased from Alfa Aesar (Haverhill, MA, USA), Fischer Scientific Company (Waltham, MA, USA), Sigma-Aldrich (St. Louis, MO, USA), and VWR International (Radnor, PA, USA). Purification of these reagents was implemented only when needed. Argon (Ar) and nitrogen (N_2) were purchased from Air Gas (Radnor, PA, USA). Solvents (SureSeal) were used as obtained and purged using an Ar atmosphere after each use. Aldehyde and amine reagents (liquid) were passed through activated alumina columns and were subjected to an Ar atmosphere treatment prior to and after each use. ¹H NMR and ¹³C NMR were recorded using a multi-nuclei JEOL 400 nuclear magnetic resonance spectrophotometer (NMR) (TEM, Tokyo, Japan). Electrospray ionization mass spectra (ESI-MS) were obtained using Agilent 100 series MSD VL (Santa Clara, CA, USA). Gas chromatography/mass spectrometry (GC-MS) was used to analyze the synthesized amide products. The GC-MS combo used was a Shimadzu QP2010 Plus and Shimadzu QP2010 ultra electron ionization (EI) detection system (Kyoto, Tapan). The stationary phase consists of a 30 m DB-5 non-polar column, and helium (He) gas is used as the carrier (mobile phase). Other GC-MS parameters to note include injection temperature (250 °C), injection volume (1.0 μL), and run-time (37.5 min). Ultraviolet-visible spectra were obtained using a Perkin Elmer Lambda 365 UV-vis (Waltham, MA, USA).

4.2. Synthesis Pincer Ligand (1)

According to the literature, ligand synthesis was performed under nitrogen (N_2) atmosphere, 2,6-pyridinedicarbonyl dichloride was dissolved in dichloromethane (DCM) and added dropwise to a solution of 2,6-diisopropylaniline and triethylamine (Et $_3$ N) [72,76]. The reaction mixture was stirred and refluxed at 50 °C for 6 h. The organic product remained in DCM and washed with aqueous solutions of 5% sodium bicarbonate (NaHCO $_3$) followed by 3% hydrochloric acid (HCl). Sodium sulfate (Na $_2$ SO $_4$) was used to remove any remaining water in the DCM mixture prior to vacuum filtration. The solvent was then removed by rota-evaporation, and the precipitated white solid was recovered. The product was recrystallized using hexanes. The resulting product was further dried overnight under

negative pressure. After collecting the product, a white flaky solid residue was collected. The mass was recorded at 687 mg, calculating an 88% yield. Characterizations for the ligand product (1) were performed via FT-IR (Supplementary Materials, S63), ¹H NMR, and ¹³C NMR (Supplementary Materials, S64).

4.3. Synthesis of Ni (II) Complex (2)

According to the literature [72,76,77], metalation of ligand was performed under N_2 atmosphere. Compound (1) was dissolved in tetrahydrofuran (THF), and solution temperature was reduced (0 °C). n-butyllithium (2.1 mol eq) was then slowly added to solution mixture. Maintaining temperature, nickel(II) dichloride glyme ($C_4H_{10}Cl_2NiO_2$) (1.1 mol eq) was added to reaction mixture 15 min after addition of base. Low temperature was further maintained as the reaction mixture stirred overnight. A liquid nitrogen cold trap was used for solvent removal, and the resulting solid was dried under negative vacuum pressure. After collecting the fine wine-red powder product, the mass was recorded at 771 mg, calculating a 93% yield. Characterizations for the nickel(II) pincer complex (2) were performed via ESI-MS negative mode, FT-IR, and 1H NMR (Supplementary Materials, S65–S67). It is believed that chlorometallated form (2) may get converted to hydroxymetallated catalyst in the presence of moisture, which may also show catalytic activity [77,78].

4.4. General Synthesis of Benzamides

Each reaction was performed in duplicate trials. Mixing of specific aldehydes and amines depended on target product and was accomplished in a one pot process. The nickel(II) complex (2) (2 mg, 3.42×10^{-3} mmol) was weighed and added to a dry Pyrex test tube, then dissolved in anhydrous DMSO (1.0 mL) transferred to the test tube with a gas-tight syringe. This solution was subjected to an initial 5 min Ar atmosphere. All ensuing molar equivalents (eq) for remaining starting materials were calculated from the initial molar amount of 2. In sequence, a 1 M solution of lithium bis-(trimethylsilyl) amide (LiHMDS) in tetrahydrofuran (THF) (100 eq, 0.342 mL, 0.342 mmol) followed by the aldehyde (1000 eq) and then corresponding amine (500 eq) reagents were added to complete the final reaction mixture. The reaction vessel was then reconnected to an Ar atmosphere. The reaction mixture was stirred at room temperature (rt) for 15 min.

Upon completion, the reaction mixture was filtered through Celite® to remove any solid particulates prior to GC–MS sample preparation for post-reaction analysis. The filtered reaction mixture (100 μL) was transferred to a GC–MS sample vial and mixed with a combination of internal standards consisting of decane (25 μL , 1.3 \times 10 $^{-4}$ mol) and a 0.53 M solution of N-benzylbenzamide in methanol (100 μL , 5.3 \times 10 $^{-4}$ mol) and diluted to the line with ethanol (1.5 mL total volume). Following GC–MS analysis, turnover numbers were calculated using peak area integration of standards and the ensuing amide products. The general reaction scheme is shown in Figure 2b.

An internal standard method was used to determine turnover numbers (TONs). The internal standard used was *N*-benzylbenzamide in methanol. Integrations of areas under the curve for internal standard peaks and product peaks were compared. After application of dilution factors, molar amounts of target products were determined. A TON was then calculated by taking the ratio of total moles of formed products and total moles of catalyst used. The method of determination of TON is described in Supplementary Materials (S69).

The amide products were then isolated via extraction. The extraction process was carried out by spiking the polar index of the DMSO reaction mixture through the addition of a small amount of water. A solution containing a 30:70 ratio of ethyl acetate to diethyl ether was then mixed with the original reaction mixture, and the product was transferred into the organic layer. The organic layer was removed by using roto-evaporator. The remaining residues were further heated at 130 $^{\circ}$ C under vacuum to obtain the final product. The amide products recovered were several white/off-white solids and oils. Mass yields were obtained and calculated to be 4–75%. 1 H and 13 C NMR spectra were performed on each of the isolated products (Supplementary Materials, S34–S62).

Catalysts 2023, 13, 1423 18 of 21

5. Conclusions and Outlook

A novel oxidative amidation protocol involving a C–N cross-coupling approach of aryl aldehydes and primary and secondary reactants catalyzed via a nickel(II) pincer complex. This nickel(II) pincer catalyst has demonstrated capabilities in C–C and C–N bond formations in our former studies. By incorporating this nickel(II) complex to work in the context of amide formations, 33 different substituted benzamide products were synthesized. Various kinetic processes and a plausible mechanistic pathway were evaluated to gain insight.

The utilities of this nickel(II) pincer complex (2) have yet to be fully explored. In the future, we would like to see further applied to other types of C–N coupling reactions and small molecule activations such as CO_2 fixation. In the context of this study, we wish to gain more insight into the exact nature of the intermediates within the mechanistic cycle and apply our process to more complex compounds on a bigger scale.

Supplementary Materials: The following supporting information can be downloaded at https://www.mdpi.com/article/10.3390/catal13111423/s1. GC-MS Supplemental Information; NMR Supplemental Information; Other Supplemental Information.

Author Contributions: A.G. conceived the research idea, designed the experiments, and contributed to interpreting the data and establishing the reaction mechanism. P.S. wrote the manuscript, performed and/or supervised each experiment, and contributed to interpreting the data and establishing the reaction mechanism. D.H., K.S., T.J., T.A. and S.C. contributed to performing the experiments and interpreting the data. A.G., P.M. and B.W. contributed to writing the manuscript and P.M helped with interpreting some of the data and establishing the mechanism. All authors have read and agreed to the published version of the manuscript.

Funding: This research was partially financially supported by the National Science Foundation (grant no. 2223984). A.G. would also like to thank AR INBRE Grant No GR013696, which was supported by the National Institute of General Medical Sciences (NIGMS) under grant number 2P20GM103429-19. P.S., K.S. and T.J. would also like to thank the UA-Little Rock Signature Experience for partially funding the research. Lastly, D.H., S.C. and T.J. would like to thank the Arkansas Division of Higher Education SURF grants for partially funding the research.

Data Availability Statement: Data are contained within the article and Supplementary Materials.

Acknowledgments: We would like to acknowledge the Chemistry Department at UA-Little Rock for all their help and support. We would also like to acknowledge the Center for Integrative Nanotechnology and Sciences at UA-Little Rock for all their help and support.

Conflicts of Interest: The authors declare no conflict of interest.

References

- Constable, D.J.C.; Dunn, P.J.; Hayler, J.D.; Humphrey, G.R.; Leazer, J.J.L.; Linderman, R.J.; Lorenz, K.; Manley, J.; Pearlman, B.A.; Wells, A.; et al. Key green chemistry research areas—A perspective from pharmaceutical manufacturers. *Green Chem.* 2007, 9, 411–420.
- 2. Góbi, S.; Magyarfalvi, G.; Tarczay, G. VCD Robustness of the Amide-I and Amide-II Vibrational Modes of Small Peptide Models. *Chirality* **2015**, 27, 625–634. [CrossRef]
- 3. Park, Y.; Kim, Y.; Chang, S. Transition Metal-Catalyzed C-H Amination: Scope, Mechanism, and Applications. *Chem. Rev.* **2017**, 117, 9247–9301. [CrossRef]
- 4. Wieland, T.; Bodanszky, M. The World of Peptides; Springer: Berlin/Heidelberg, Germany, 1991.
- 5. Arregui, M.C.; Sánchez, D.; Althaus, R.; Scotta, R.R.; Bertolaccini, I. Assessing the risk of pesticide environmental impact in several Argentinian cropping systems with a fuzzy expert indicator. *Pest Manag. Sci.* **2010**, *66*, 736–740. [CrossRef]
- Hartwig, J.F. Carbon-heteroatom bond formation catalysed by organometallic complexes. Nature 2008, 455, 314–322. [CrossRef]
- 7. Liu, C.; Szostak, M. Decarbonylative cross-coupling of amides. Org. Biomol. Chem. 2018, 16, 7998–8010. [CrossRef]
- 8. Lanigan, R.M.; Sheppard, T.D. Recent Developments in Amide Synthesis: Direct Amidation of Carboxylic Acids and Transamidation Reactions. *Eur. J. Org. Chem.* **2013**, 2013, 7453–7465. [CrossRef]
- 9. Capparelli, E.V.; Holland, D.; Okamoto, C.; Gragg, B.; Durelle, J.; Marquie-Beck, J.; Van den Brande, G.; Ellis, R.; Letendre, S. Lopinavir concentrations in cerebrospinal fluid exceed the 50% inhibitory concentration for HIV. *AIDS* **2005**, *19*, 949–952. [CrossRef]
- 10. Pattabiraman, V.R.; Bode, J.W. Rethinking amide bond synthesis. Nature 2011, 480, 471–479. [CrossRef]

Catalysts 2023, 13, 1423 19 of 21

11. Lu, B.; Xiao, W.-J.; Chen, J.-R. Recent Advances in Visible-Light-Mediated Amide Synthesis. Molecules 2022, 27, 517. [CrossRef]

- 12. Valeur, E.; Bradley, M. Amide bond formation: Beyond the myth of coupling reagents. *Chem. Soc. Rev.* **2009**, *38*, 606–631. [CrossRef]
- 13. Bates, R. Organic Synthesis Using Transition Metals; Wiley: Hoboken, NJ, USA, 2012.
- 14. de Figueiredo, R.M.; Suppo, J.-S.; Campagne, J.-M. Nonclassical Routes for Amide Bond Formation. *Chem. Rev.* **2016**, *116*, 12029–12122. [CrossRef] [PubMed]
- 15. Jiang, Y.Y.; Zhu, L.; Liang, Y.; Man, X.; Bi, S. Mechanism of Amide Bond Formation from Carboxylic Acids and Amines Promoted by 9-Silafluorenyl Dichloride Derivatives. *J. Org. Chem.* **2017**, *82*, 9087–9096. [CrossRef]
- 16. Trost, B.M. Atom Economy—A Challenge for Organic Synthesis: Homogeneous Catalysis Leads the Way. In *Angewandte Chemie International Edition in English*; John Wiley & Sons, Ltd.: Hoboken, NJ, USA, 1995; Volume 34, pp. 259–281.
- 17. Brennführer, A.; Neumann, H.; Beller, M. Palladium-Catalyzed Carbonylation Reactions of Aryl Halides and Related Compounds. *Angew. Chem. Int. Ed.* **2009**, *48*, 4114–4133. [CrossRef] [PubMed]
- Ishihara, K.; Ohara, S.; Yamamoto, H. 3,4,5-Trifluorobenzeneboronic Acid as an Extremely Active Amidation Catalyst. J. Org. Chem. 1996, 61, 4196–4197. [CrossRef]
- 19. Ali, A.; Siddiki, S.M.A.H.; Kon, K.; Shimizu, K.-I. A Heterogeneous Niobium(V) Oxide Catalyst for the Direct Amidation of Esters. *ChemCatChem* **2015**, *7*, 2705–2710. [CrossRef]
- 20. Lundberg, H.; Tinnis, F.; Adolfsson, H. Direct Amide Coupling of Non-activated Carboxylic Acids and Amines Catalysed by Zirconium(IV) Chloride. *Chem.-A Eur. J.* **2012**, *18*, 3822–3826. [CrossRef]
- Lundberg, H.; Adolfsson, H. Hafnium-Catalyzed Direct Amide Formation at Room Temperature. ACS Catal. 2015, 5, 3271–3277.
 [CrossRef]
- 22. Shu, W.; Liu, M.S. Catalytic, metal-free amide synthesis from aldehydes and imines enabled by a dual-catalyzed umpolung strategy under redox-neutral conditions. *ACS Catal.* **2020**, *10*, 12960–12966.
- 23. List, B. Introduction: Organocatalysis. Chem. Rev. 2007, 107, 5413–5415. [CrossRef]
- 24. Lenstra, D.C.; Rutjes, F.P.J.T.; Mecinović, J. Triphenylphosphine-catalysed amide bond formation between carboxylic acids and amines. *Chem. Commun.* **2014**, *50*, *5763*–*5766*. [CrossRef]
- 25. Hamstra, D.F.J.; Lenstra, D.C.; Koenders, T.J.; Rutjes, F.P.J.T.; Mecinović, J. Poly(methylhydrosiloxane) as a green reducing agent in organophosphorus-catalysed amide bond formation. *Org. Biomol. Chem.* **2017**, *15*, 6426–6432. [CrossRef]
- 26. Akondi, S.M.; Gangireddy, P.; Pickel, T.C.; Liebeskind, L.S. Aerobic, Diselenide-Catalyzed Redox Dehydration: Amides and Peptides. Org. Lett. 2018, 20, 538–541. [CrossRef]
- 27. Handoko, N.; Panigrahi, R.; Arora, P.S. Two-Component Redox Organocatalyst for Peptide Bond Formation. *J. Am. Chem. Soc.* **2022**, 144, 3637–3643. [CrossRef]
- 28. Nguyen, T.V.; Lyons, D.J.M. A novel aromatic carbocation-based coupling reagent for esterification and amidation reactions. *Chem. Commun.* **2015**, *51*, 3131–3134. [CrossRef]
- 29. Nordstrøm, L.U.; Vogt, H.; Madsen, R. Amide Synthesis from Alcohols and Amines by the Extrusion of Dihydrogen. *J. Am. Chem. Soc.* 2008, 130, 17672–17673. [CrossRef]
- 30. Tillack, A.; Rudloff, I.; Beller, M. Catalytic Amination of Aldehydes to Amides. Eur. J. Org. Chem. 2001, 3, 523-528. [CrossRef]
- 31. Gunanathan, C.; Ben-David, Y.; Milstein, D. Direct Synthesis of Amides from Alcohols and Amines with Liberation of H₂. *Science* **2007**, *317*, 790–792. [CrossRef]
- 32. Capeness, M.; Edmundson, M.; Horsfall, L. Nickel and platinum group metal nanoparticle production by Desulfovibrio alaskensis G20. *New Biotechnol.* **2015**, *32*, 727–731. [CrossRef]
- 33. Chirik, P.; Morris, R. Getting Down to Earth: The Renaissance of Catalysis with Abundant Metals. *Acc. Chem. Res.* **2015**, *48*, 2495. [CrossRef]
- 34. Soulé, J.F.; Miyamura, H.; Kobayashi, S. Powerful amide synthesis from alcohols and amines under aerobic conditions catalyzed by gold or gold/iron, -nickel or-cobalt nanoparticles. *J. Am. Chem. Soc.* **2011**, *133*, 18550–18553. [CrossRef] [PubMed]
- 35. Whittaker, A.M.; Dong, V.M. Nickel-Catalyzed Dehydrogenative Cross-Coupling: Direct Transformation of Aldehydes into Esters and Amides. *Angew. Chem. Int. Ed.* **2015**, *54*, 1312–1315. [CrossRef] [PubMed]
- 36. Alandini, N.; Buzzetti, L.; Favi, G.; Schulte, T.; Candish, L.; Collins, K.D.; Melchiorre, P. Amide Synthesis by Nickel/Photoredox-Catalyzed Direct Carbamoylation of (Hetero)Aryl Bromides. *Angew. Chem.* **2020**, *132*, 5286–5291. [CrossRef]
- 37. Yan, Z.; Liu, F.; Wang, X.; Qiang, Q.; Li, Y.; Zhang, Y.; Rong, Z.-Q. Redox-neutral dehydrogenative cross-coupling of alcohols and amines enabled by nickel catalysis. *Org. Chem. Front.* **2022**, *9*, 1703–1710. [CrossRef]
- 38. Sang, J.W.; Li, Q.; Zhang, C.; Zhang, Y.; Wang, J.; Zhang, W.D. Nickel/Photoredox-Catalyzed Direct Amidation of Aldehydes with Nitroarenes via Fully Catalytic Process. *Org. Lett.* **2023**, *25*, 4592–4597. [CrossRef] [PubMed]
- 39. Goel, B.; Vyas, V.; Tripathi, N.; Singh, A.K.; Menezes, P.W.; Indra, A.; Jain, S.K. Amidation of Aldehydes with Amines under Mild Conditions Using Metal-Organic Framework Derived NiO@Ni Mott-Schottky Catalyst. *ChemCatChem* **2020**, *12*, 5743–5749. [CrossRef]
- 40. Mennen, S.M.; Alhambra, C.; Allen, C.L.; Barberis, M.; Berritt, S.; Brandt, T.A.; Campbell, A.D.; Castañón, J.; Cherney, A.H.; Chritensen, M.; et al. The Evolution of High-Throughput Experimentation in Pharmaceutical Development and Perspectives on the Future. *Org. Process Res. Dev.* **2019**, 23, 1213–1242. [CrossRef]

Catalysts 2023, 13, 1423 20 of 21

41. Gartia, Y.; Ramidi, P.; Jones, D.E.; Pulla, S.; Ghosh, A. Nickel Complex Catalyzed Efficient Activation of sp3 and sp2 C–H Bonds for Alkylation and Arylation of Oxygen Containing Heterocyclic Molecules. *Catal. Lett.* **2014**, *144*, 507–515. [CrossRef]

- 42. Gartia, Y.; Pulla, S.; Ramidi, P.; Farris, C.C.; Nima, Z.; Jones, D.E.; Biris, A.S.; Ghosh, A. A Novel Iron Complex for Cross-Coupling Reactions of Multiple C–Cl Bonds in Polychlorinated Solvents with Grignard Reagents. *Catal. Lett.* **2012**, 142, 1397–1404. [CrossRef]
- 43. Albkuri, Y.M.; RanguMagar, A.B.; Brandt, A.; Wayland, H.A.; Chhetri, B.P.; Parnell, C.M.; Szwedo, P.; Parameswaran-Thankam, A.; Ghosh, A. C–N Cross-coupling Reactions of Amines with Aryl Halides Using Amide-Based Pincer Nickel(II) Catalyst. *Catal. Lett.* 2020, 150, 1669–1678. [CrossRef]
- 44. Brandt, A.; RanguMagar, A.B.; Szwedo, P.; Wayland, H.A.; Parnell, C.M.; Munshi, P.; Ghosh, A. Highly economical and direct amination of sp3 carbon using low-cost nickel pincer catalyst. *RSC Adv.* **2021**, *11*, 1862–1874. [CrossRef] [PubMed]
- 45. Bordwell, F.G. Equilibrium acidities in dimethyl sulfoxide solution. Acc. Chem. Res. 1988, 21, 456–463. [CrossRef]
- 46. Fraser, R.R.; Mansour, T.S. Acidity measurements with lithiated amines: Steric reduction and electronic enhancement of acidity. *J. Org. Chem.* **1984**, *49*, 3442–3443. [CrossRef]
- 47. Fraser, R.R.; Mansour, T.S.; Savard, S. Acidity measurements on pyridines in tetrahydrofuran using lithiated silylamines. *J. Org. Chem.* **1985**, *50*, 3232–3234. [CrossRef]
- 48. Bordwell, F.G.; Algrim, D.; Vanier, N.R. Acidities of anilines and toluenes. J. Org. Chem. 1977, 42, 1817–1819. [CrossRef]
- 49. Munshi, P.; Main, A.D.; Linehan, J.C.; Tai, C.-C.; Jessop, P.G. Hydrogenation of Carbon Dioxide Catalyzed by Ruthenium Trimethylphosphine Complexes: The Accelerating Effect of Certain Alcohols and Amines. *J. Am. Chem. Soc.* **2002**, 124, 7963–7971. [CrossRef]
- 50. Zhang, T.; Zhong, K.; Lin, Z.K.; Niu, L.; Li, Z.Q.; Bai, R.; Engle, K.M.; Lan, Y. Revised Mechanism of C(sp3)-C(sp3) Reductive Elimination from Ni(II) with the Assistance of a Z-Type Metalloligand. *J. Am. Chem. Soc.* **2023**, 145, 2207–2218. [CrossRef]
- 51. Reyes, A.; Scott, R.M. Specific effects of dimethyl sulfoxide on the relative basicities of aliphatic amines. *J. Phys. Chem.* **1980**, *84*, 3600–3603. [CrossRef]
- 52. Kozuch, S.; Martin, J.M.L. "Turning Over" Definitions in Catalytic Cycles. Acc. Catal. 2012, 2, 2787–2794. [CrossRef]
- 53. Lente, G. Comment on "Turning Over" Definitions in Catalytic Cycles. Acc. Catal. 2013, 3, 381–382. [CrossRef]
- 54. Wheeler, S.E. Understanding Substituent Effects in Noncovalent Interactions Involving Aromatic Rings. *Accounts Chem. Res.* **2013**, 46, 1029–1038. [CrossRef]
- 55. Pérez, P.; Domingo, L.R.; Duque-Noreña, M.; Chamorro, E. A condensed-to-atom nucleophilicity index. An application to the director effects on the electrophilic aromatic substitutions. *J. Mol. Struct. THEOCHEM* **2008**, *895*, 86–91. [CrossRef]
- 56. Rosenthal, J.; Schuster, D.I. The Anomalous Reactivity of Fluorobenzene in Electrophilic Aromatic Substitution and Related Phenomena. *J. Chem. Educ.* **2003**, *80*, 679–690. [CrossRef]
- 57. Matulis, D.; Bloomfield, V.A. Thermodynamics of the hydrophobic effect. I. Coupling of aggregation and pKa shifts in solutions of aliphatic amines. *Biophys. Chem.* **2001**, *93*, 37–51. [CrossRef] [PubMed]
- 58. Brotzel, F.; Ying, C.C.; Mayr, H. Nucleophilicities of primary and secondary amines in water. *J. Org. Chem.* **2007**, *72*, 3679–3688. [CrossRef]
- 59. Lanigan, R.M.; Starkov, P.; Sheppard, T.D. Direct synthesis of amides from carboxylic acids and amines using B(OCH₂CF₃)₃. *J. Org. Chem.* **2013**, *78*, 4512–4523. [CrossRef]
- 60. Schuhmacher, A.; Shiro, T.; Ryan, S.J.; Bode, J.W. Synthesis of secondary and tertiary amides without coupling agents from amines and potassium acyltrifluoroborates (KATs). *Chem. Sci.* **2020**, *11*, 7609–7614. [CrossRef]
- 61. Henderson, W.A.; Schultz, C.J. The Nucleophilicity of Amines. J. Org. Chem. 1962, 27, 4643–4646. [CrossRef]
- 62. Nystrom, R.F.; Brown, W.G. Reduction of Organic Compounds by Lithium Aluminum Hydride. I. Aldehydes, Ketones, Esters, Acid Chlorides and Acid Anhydrides. *J. Am. Chem. Soc.* **1947**, *69*, 1197–1199. [CrossRef]
- 63. Brown, H.C.; Wheeler, O.H.; Ichikawa, K. Chemical effects of steric strains—XIII: Kinetics of the reaction of sodium borohydride with carbonyl groups—A convenient tool for investigating the reactivities of aldehydes and ketones. *Tetrahedron* **1957**, *1*, 214–220. [CrossRef]
- 64. Ge, S.; Green, R.A.; Hartwig, J.F. Controlling First-Row Catalysts: Amination of Aryl and Heteroaryl Chlorides and Bromides with Primary Aliphatic Amines Catalyzed by a BINAP-Ligated Single-Component Ni⁰ Complex. *J. Am. Chem. Soc.* **2014**, *136*, 1617–1627. [CrossRef] [PubMed]
- 65. Chang, R. Physical Chemistry for the Biosciences; University Science Books: Herndon, VA, USA, 2005.
- 66. Nicolas, E.; Ohleier, A.F.; D'Accriscio; Pécharman, A.F.; Demange, M.; Ribagnac, J.; Ballester, J.; Gosmini, C.; Mézailles, N. '(Diphosphine)Nickel'-Catalyzed Negishi Cross-Coupling: An Experimental and Theoretical Study. *Chem.-A Eur. J.* **2015**, 21, 7690–7694. [CrossRef] [PubMed]
- 67. Chong, E.; Kampf, J.W.; Ariafard, A.; Canty, A.J.; Sanford, M.S. Oxidatively Induced C–H Activation at High Valent Nickel. *J. Am. Chem. Soc.* **2017**, 139, 6058–6061. [CrossRef] [PubMed]
- 68. Weires, N.A.; Caspi, D.D.; Garg, N.K. Kinetic Modeling of the Nickel-Catalyzed Esterification of Amides. *ACS Catal.* **2017**, 7, 4381–4385. [CrossRef]
- 69. Dander, J.E.; Garg, N.K. Breaking Amides using Nickel Catalysis. ACS Catal. 2017, 7, 1413–1423. [CrossRef]

Catalysts 2023, 13, 1423 21 of 21

70. Beromi, M.M.; Nova, A.; Balcells, D.; Brasacchio, A.M.; Brudvig, G.W.; Guard, L.M.; Hazari, N.; Vinyard, D.J. Mechanistic Study of an Improved Ni Precatalyst for Suzuki–Miyaura Reactions of Aryl Sulfamates: Understanding the Role of Ni(I) Species. *J. Am. Chem. Soc.* 2017, 139, 922–936. [CrossRef]

- 71. Shi, S.; Meng, G.; Szostak, M. Synthesis of Biaryls through Nickel-Catalyzed Suzuki-Miyaura Coupling of Amides by Carbon-Nitrogen Bond Cleavage. *Angew. Chem. Int. Ed.* **2016**, *55*, 6959–6963. [CrossRef]
- 72. Wasilke, J.C.; Wu, G.; Bu, X.; Kehr, G.; Erker, G. Ruthenium carbene complexes featuring a tridentate pincer-type ligand. *Organometallics* **2005**, 24, 4289–4297. [CrossRef]
- 73. Gartia, Y.; Ramidi, P.; Cheerla, S.; Felton, C.M.; Jones, D.E.; Das, B.C.; Ghosh, A. Activation of sp3 and sp2 CH bonds of oxygen containing heterocyclic molecules for alkylation and arylation reactions catalyzed by an iron complex. *J. Mol. Catal. A Chem.* **2014**, 392, 253–259. [CrossRef]
- 74. Zheng, B.; Tang, F.; Luo, J.; Schultz, J.W.; Rath, N.P.; Mirica, L.M. Organometallic Nickel(III) Complexes Relevant to Cross-Coupling and Carbon–Heteroatom Bond Formation Reactions. *J. Am. Chem. Soc.* **2014**, *136*, 6499–6504. [CrossRef]
- 75. Kozuch, S.; Lee, S.E.; Shaik, S. Theoretical Analysis of the Catalytic Cycle of a Nickel Cross-Coupling Process: Application of the Energetic Span Model. *Organometallics* **2009**, *28*, 1303–1308. [CrossRef]
- 76. Liu, H.; Jia, X.; Wang, F.; Dai, Q.; Wang, B.; Bi, J.; Zhang, C.; Zhao, L.; Bai, C.; Hu, Y.; et al. Synthesis of bis(*N*-arylcarboximidoylchloride)pyridine cobalt(ii) complexes and their catalytic behavior for 1,3-butadiene polymerization. *Dalt. Trans.* 2013, 42, 13723. [CrossRef] [PubMed]
- 77. Huang, D.; Holm, R.H. Reactions of the terminal Ni(II)-OH group in substitution and electrophilic reactions with carbon dioxide and other substrates: Structural definition of binding modes in an intramolecular Ni(II)Fe(II) bridged site. *J. Am. Chem. Soc.* 2010, 132, 4693–4701. [CrossRef] [PubMed]
- 78. Lefèvre, X.; Spasyuk, D.M.; Zargarian, D. New POCOP-type pincer complexes of Nickel(II). *J. Organomet. Chem.* **2011**, 696, 864–870. [CrossRef]

Disclaimer/Publisher's Note: The statements, opinions and data contained in all publications are solely those of the individual author(s) and contributor(s) and not of MDPI and/or the editor(s). MDPI and/or the editor(s) disclaim responsibility for any injury to people or property resulting from any ideas, methods, instructions or products referred to in the content.